RESEARCH NOTES FROM COLLABORATIONS

Signals of Models with Large Extra Dimensions in ATLAS

L Vacavant and I Hinchliffe

Lawrence Berkeley National Laboratory, Physics Division, 1 Cyclotron Road, Berkeley CA 94720, USA

Abstract. The generic missing transverse energy signals at LHC for theories having large extra dimensions are discussed. Final states of jets plus missing energy and photons plus missing energy are simulated in the ATLAS detector. The discovery limit of LHC and the methods to determine the parameters of the underlying model are discussed.

SN-ATLAS-2001-005
10 May 2001

Submitted to: *J. Phys. G: Nucl. Part. Phys.*

1. Introduction

There is much recent theoretical interest in models of particle physics that have extra-dimensions in addition to the 3+1 dimensions of normal space-time [1, 2]. In these models, new physics can appear at a mass scale of order 1 TeV and can therefore be accessible at LHC. The standard model has a large hierarchy of scales that exists between the mass scale of the weak interactions, set by the Fermi constant G_F (or the W-mass, M_W), and that of gravity, set by Newton's constant G_N (or the Planck Mass. $M_P \sim 10^{19}$ GeV). It is believed that a consistent quantum theory of gravity must be a string theory [3] which requires additional dimensions in order to be self-consistent. String theory has some inherent scale, the string scale M_S, associated with it. The additional dimensions must be compactified on some scale R so that they are currently unobserved. It is often assumed that $M_s \sim M_P \sim 1/R$ so that new physics would not be visible until these huge energy scales are reached. This type of model offers no insight as to the origin of the large hierarchy although it can, since the theory is supersymmetric, ensure that the hierarchy is stable with respect to quantum corrections.

Recently however it has been suggested that R could be much larger, allowing the fundamental scale of gravity, here called M_D, to be close to M_W and so remove the large hierarchy of scales[1]. If there are δ additional dimensions of size R, then the observed Newton constant is related to the fundamental scale M_D by

$$G_N^{-1} = 8\pi R^{\delta} M_D^{2+\delta}$$

If $M_D \sim 1$ TeV then $R \sim 10^{32/\delta - 16}$ mm implying that, if $\delta \geq 2$, R is smaller than the scales of order 1 mm down to which gravitational interactions have been probed. In this picture the apparent weakness of observed gravity is due to its dilution by

the spreading of its field into the additional dimensions. It should be noted that the hierarchy problem is not solved in the simplest implementation of the idea; the large ratio M_P/M_W is replaced by the large value of RM_D whose origin is not explained.

When an extra dimension is compactified on a circle with size R, particles propagating exclusively in the extra dimensions appear, from a four dimensional viewpoint, as a tower of massive states. The characteristic mass splitting of these (Kaluza-Klein) states is of order $1/R$. In particular, gravitons propagating in the extra dimensions will appear to be massive states whose coupling to ordinary matter is determined only by gravitational interactions and is therefore known. However, the Standard model particles cannot be allowed to propagate into the extra dimensions as there is no "excited electron" with a mass below 100 GeV. New physics is expected to appear at a scale M_D; the details of this physics are model dependent.

This paper is concerned primarily with the model independent signatures involving the emission of graviton resonances and their observability in the ATLAS detector.

2. Graviton direct production

The emission of gravitons in particle collisions is calculable in terms of the universal coupling of gravity to all matter (G_N). The calculations become unreliable once energies comparable to the fundamental scale of gravity are reached. (Similarly, calculations in the Fermi theory of weak interactions become unreliable at energy scales of order M_W.) In the Standard Model, this energy is M_P, in the models with extra dimensions, it is M_D. In addition to the emission of massless gravitons, the Kaluza-Klein excitations that have mass differences of order $1/R$ can also be emitted and their rate calculated as their coupling to ordinary matter is also determined. For experiments involving the collision of particles whose energy is much larger than this mass splitting, the discrete spectrum can be approximated by a continuum with a density of states $dN/dm \sim m^{\delta-1}$. Since these emitted gravitons interact very weakly with ordinary matter, their emission gives rise to missing transverse energy signatures.

2.1. Sub-processes and cross-section

The relevant processes for LHC are $gg \to gG$, $qg \to qG$ and $q\overline{q} \to Gg$ which give rise to final states of jets plus missing transverse energy ($\not{E}_T$) and $q\overline{q} \to G\gamma$ which gives rise to final states with a photon plus $\not{E}_T$. Final states of $Z + \not{E}_T$ are not considered as the effective rates are much lower since the Z can only be observed at LHC via its leptonic decay.

The relevant partonic cross sections can be written in the form $\frac{d^2\sigma}{dtdm}$ where m is the mass of the recoiling graviton and $t = (p_a - p_f)^2$ is the usual Mandelstam variable (a represents an incoming parton and f the outgoing quark, gluon or photon). The differential cross-section can be expressed in the following form:

$$\frac{d^4\sigma}{dm^2 dp^2_{T_{jet,\gamma}} dy_{jet,\gamma} dy_G} = \frac{m_G^{\delta-2}}{2} \frac{S_{\delta-1}}{M_D^{\delta+2}} \frac{d\sigma_m}{dt} \sum_{i,j} \frac{f_i(x_1)}{x_1} \frac{f_j(x_2)}{x_2} \qquad (1)$$

where the partonic cross-sections $\frac{d\sigma_m}{dt}$ are given by [4] (eqs. 64-67)‡. $S_{\delta-1}$ is the surface of a unit-radius sphere in δ dimensions and $f_i(x)$ are the parton structure

‡ The cancellation of the $\bar{M}_P^2$ factor has already been taken into account in eq. 1

functions. It is important to notice that the fundamental scale M_D is factorized in Eqn. 1: $\sigma \propto M_D^{-\delta-2}$.

2.2. Implementation in ISAJET

For the purposes of this simulation, the relevant subprocesses have been implemented in ISAJET [5, 6] and are available in versions 7.47 and later. The implementation is modeled on that of $W + jet$, the mass spectrum being adjusted to reflect the tower of graviton states rather than the virtual W. The user has to provide the generator with a set of six parameters: the number of extra-dimensions, the mass scale and the transverse momentum and mass ranges of the produced graviton. In addition a logical flag UVCUT can be set to implement a cut-off in the cross-section for large values of the partonic center of mass energy. This cut-off is required as the cross-section is not valid at high energy. If the result depends strongly on this cut-off, then the resulting rates are sensitive to physics above the scale M_D and the calculations are unreliable. This is discussed in more detail in section 2.4.

2.3. Parameter ranges

The model has two parameters, the number of extra-dimensions δ and the fundamental scale M_D, for which some constraints already exist. The reader is referred to reference [4] and references therein for further details. The case $\delta = 1$ is already excluded since it would imply deviations of the Newton law of gravitational attraction at distance scales that have already been explored. The case $\delta = 2$ is not very likely because of cosmological arguments. In particular graviton emission from Supernova 1987a [7] implies that $M_D > 50$ TeV. Large values of δ (> 6) can not be probed at LHC because the cross-section for graviton emission is too small. The lower value of M_D that can be considered is determined by two factors. It should be larger than the current direct limit from similar processes at the Tevatron. Furthermore it should also be large enough so that there are no significant contributions from the parton-parton center of mass energies where the effective theory is not appropriate, as discussed in the next section.

2.4. Effective theory and validity range for M_D

It is important to note that the theory [4] is an effective low-energy theory, valid below the fundamental scale M_D. The behavior above M_D is not known, neither is the exact scale at which the theory breaks down. The prescription in reference [4] has been used to assess the applicability of the effective theory: we checked whether the standard cross-section for the process is comparable to the truncated one where contributions from the high energy region are suppressed. By comparing the results obtained by using equation 1 with those from the truncated form, the region of parameters where the results are reliable can be determined; if the results are the same then there is no sensitivity to the high energy region where new physics must enter.

In reference [4] the partonic cross-section is truncated by setting it to zero when the partonic center of mass energy ($\sqrt{\hat{s}}$) exceeds M_D: this is a worst case scenario which is not physical and is difficult to implement in a generator. Hence in the ISAJET implementation a less drastic approach (referred to in the following as "soft truncature") is taken; if the variable UVCUT is set then the rate given by equation

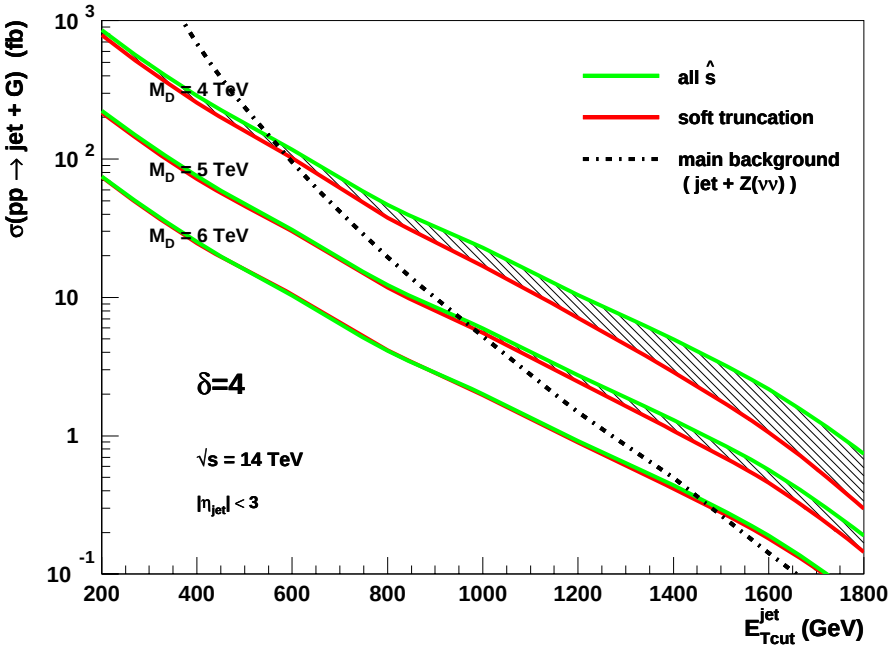

Figure 1. Integrated cross-section $\int_{E_T^{cut}}(d\sigma/dE_T)dE_T$ for the extra-dimensions processes leading to the production of a jet of transverse energy E_T in association with missing energy, in the case of four extra-dimensions and for various values of M_D. The hatched regions correspond to regions in the (E_T^{cut}, M_D) plane where no model independent prediction is possible (cf. § 2.4 for details).

1 is reduced by a factor of $M_D^4/\hat{s}^2$ when $\hat{s} > M_D^2$. This ensures that the cross-section satisfies unitarity constraints.

For fixed values of M_D and δ there is a maximum value of jet (photon) E_T for which the results are reliable. Alternatively, for a fixed number of expected events or fixed value of E_T^{cut}, there is a value of M_D below which the results are not reliable. If a significant number of events is expected in this region where the truncated and untruncated models disagree, then the experiment is sensitive to new physics appearing at scales M_D and one can expect that other signals will appear. As an illustration, figure 1 shows the event rate for the $jet + G$ production for $\delta = 4$ as a function of the cut on the jet transverse energy. For each value of M_D, the upper curve shows the cross-section while the lower one shows the softly truncated cross-section. For $E_T^{cut} = 1$ TeV, the two curves disagree if $M_D = 4$ TeV but the agreement improves with larger values of M_D: therefore in this case the minimal value of M_D for which model independent prediction is possible is approximately 5 TeV.

3. Study

3.1. Generation

All the signals studied here have been generated using the ISAJET implementation of the extra-dimension process with the default set of structure functions (CTEQ3L [8]). Each signal sample consists of 60k events generated in $p_T^{jet,\gamma}$ bins and re-weighted. Most of the background samples have been generated in the same way with ISAJET and contain each 300k events.

3.2. Detector simulation

The ATLAS detector is a general-purpose experiment at the LHC whose features and performance are described in reference [9]. Its main features with respect to this analysis are: a full-coverage hadronic calorimetry up to $|\eta| < 4.9$ for accurate jet and missing energy measurements, an excellent electromagnetic calorimetry for photon identification and measurements as well as very good identification and measurements of electrons and muons. A fast particle-level simulation of the detector, ATLFAST [10], provides a realistic simulation of the most crucial detector aspects and has been used for this study.

3.3. Analysis and signal observability

Unless otherwise stated, the results will be given for an integrated luminosity of 100 fb^{-1}, which is expected to be collected after one year of data taking at the nominal luminosity of the LHC.

The first pass of the selection emulates the trigger, based on the foreseen trigger menus for Level 1 and Level 2 [11, 12, 13]. Then the offline analysis is applied. This selection is kept simple given the inherent uncertainties on the tools used for physics modeling.

To define the signal observability, two statistical estimators are defined. $\mathcal{S}_{max} = S/\sqrt{B}$ is a rather naive estimator where S (B) is the expected number of signal (background) events. It is a bit optimistic and can be seen as a upper limit on the sensitivity. The other estimator, $\mathcal{S}_{min}$, is defined in a very conservative way: for each signal, the main background (invisible decays of the Z) is estimated using a calibration sample of electronic and muonic decays of the Z. The ratio α of the number of events in the calibration sample to the number of expected background, taking into account the relative acceptance, is incorporated into the estimator as $\mathcal{S}_{min} = S/\sqrt{\alpha B}$. This is a worst case scenario; in practice the many measurements at LHC will give one confidence in predicting the missing transverse energy rate in the signal region.

4. Single jet signature

The signal $pp \to jet + \not{E}_T$ is the most promising one for the direct graviton production at LHC. The dominant sub-process is $qg \to qG$. The cases with $\delta = 2, 3, 4$ have been studied.

4.1. Effective theory and validity range

Following the method described in § 2.4, we found that the approximate minimal values of M_D are 4, 4.5 and 5 TeV for $\delta = 2, 3$ and 4. For more than four extra-dimensions, the rates are too low in the regions where the calculation is reliable.

4.2. Backgrounds

At the large values of missing E_T that are being considered, the dominant backgrounds arise from processes that can give rise to neutrinos in the final state, *viz.* $jet{+}Z(\rightarrow \nu\nu)$, $jet + W(\rightarrow \tau\nu)$, $jet + W(\rightarrow \mu\nu)$ and $jet + W(\rightarrow e\nu)$. We veto events where there is an isolated lepton within the acceptance of the ATLAS muon or tracking systems as this reduces the background from the last two sources. Additional instrumental background can arise from events where jet energies are badly measured or energy is lost in cracks or beyond the end of the calorimeter. Studies [14] have shown that this effect is very small for large values of missing E_T that are relevant here and we neglect it.

4.3. Event selection and analysis

After the trigger selection, the lepton veto is applied. Additional selection relies on the topology of the events: missing transverse momentum, missing transverse momentum and leading jet back-to-back. A cut to remove the hadronic decays of the τ is also described.

4.3.1. Trigger The trigger is based on a combination of missing energy and jet. At low luminosity, a jet within the trigger acceptance ($|\eta| < 3.2$) and with $p_T \geq 50$ GeV/c is required, in addition to at least 50 GeV of missing transverse energy. At high luminosity, both thresholds are raised to 100 GeV. If needed, a higher threshold for $\not\!\!E_T$ could be used without affecting the study since the extraction of the signal relies on event rates at very large values of $\not\!\!E_T$ (of the order of one TeV).

4.3.2. Lepton veto Events with an isolated lepton are vetoed, mainly to reduce the contribution of the jet+W background where the W decays leptonically. The acceptance for such isolated leptons is defined as follows: $p_T > 5$ (resp. 6) GeV/c and $|\eta| < 2.5$ for an electron (resp. muon).

A conservative value of $\epsilon_{veto} = 98\%$ for the lepton veto efficiency has been included by re-weighting the events by $(1 - \epsilon_{veto})^{n_{leptons}}$. No provision has been made for difference in the identification efficiency for electrons and muons. The veto retains 99.8% of the signal events while rejecting 23.3%, 74.3% and 61.1% of the $jW(\tau)$, $jW(e)$ and $jW(\mu)$ background events respectively.

4.3.3. Topology The topology of the graviton+jet signal is quite simple: a mono-jet which is back-to-back in azimuth to balancing missing transverse momentum. Additional jets arise from initial and final state QCD radiation. In the background events, a W or Z is emitted whereas in the signal events it is one of the tower of gravitons. The mass of this graviton can be large as the density of states increases exponentially with the mass and a typical emission can therefore have a mass larger than that of the W. The amount of QCD radiation is controlled by the total energy

in the partonic system. For production at fixed E_T, we expect that there is more energy in the signal process due to the larger mass and therefore more QCD radiation which should manifest itself in increased jet multiplicity. In addition the backgrounds arise from initial states consisting mainly of quark-gluon collisions, whereas the signal receives contributions from gluon-gluon initial states. The greater color charge of the latter again tends to produce more radiation in the signal events.

These effects can be seen in the distribution of the number of jets, slightly higher in signal events than in background events; as well as in distribution of the azimuthal angle difference between the leading jet and the missing transverse momentum. However these differences between signal and backgrounds are diminished when events with large $\not\!\!E_T$ are selected (the relevant plots can be seen in reference [15]). Therefore and for the simplicity of the analysis no cut has been applied on these quantities.

In the signal events and in most of the backgrounds, the second jet is predominantly localized in the opposite hemisphere of the missing transverse energy: the leading jet as well as the other ones induced by gluon radiations and $\vec{\not\!\!p}_T$ are back-to-back in azimuth. However this is not the case in the $jet + W(\rightarrow \tau\nu)$ events, where hadronic decays of the taus can induce some hadronic activity on the same side of the missing momentum. This feature remains after a large cut on the missing transverse energy and can be used to reduce the background from $W \rightarrow \tau\nu$. A cut $\delta\phi(\vec{\not\!\!p}_T, jet_2) \geq 0.5$ is applied and rejects 6% of the signal events, 27% of the $jW(\tau\nu)$ events and 11% of all the background.

Finally, figure 2 shows the missing transverse energy distribution of the backgrounds and of the signals for several choices of δ and M_D after this selection. The signal emerges from the background at large $\not\!\!E_T$. The distributions for the different signals reflect the expected scaling of the cross-section as a function of $M_D^{-\delta-2}$.

4.4. Signal significance

After a typical cut $\not\!\!E_T > 1$ TeV, the number of remaining background events are shown in table 1 while the number of signal events and the statistical significances are shown in table 2.

To estimate the conservative significance, the ratio between the background, dominated by the $jZ(\nu\nu)$ events, and the calibration sample has been studied by simulating and applying a basic selection on $jZ(\rightarrow ee)$ events. For triggering we required one jet of at least 50 (100) GeV at low (high) luminosity within the trigger acceptance ($|\eta| < 3.2$) and two isolated electrons of at least 15 (20) GeV within $|\eta| < 2.5$. The invariant mass of the two electrons is required to lie in $m_Z \pm 10$ GeV. Assuming that the $jZ(\rightarrow \mu\mu)$ sample can also be used, the calibration sample is approximately a factor of 7 smaller than the background sample. We therefore used $\mathcal{S}_{min} = S/\sqrt{7B}$ as the conservative statistical estimator.

4.5. Sensitivity

The maximum reach in M_D is shown in figure 3 as a function of the cut on the jet E_T ($\sim \not\!\!E_T$). The estimators $\mathcal{S}_{min}$ and $\mathcal{S}_{max}$ are shown and in both cases a 5-sigma significance and at least 100 signal events are required. For two extra-dimensions, it can be seen that some sensitivity could be gained by loosening the cut on $\not\!\!E_T$ below the 1 TeV cut we applied. However the background in this region is less under control.

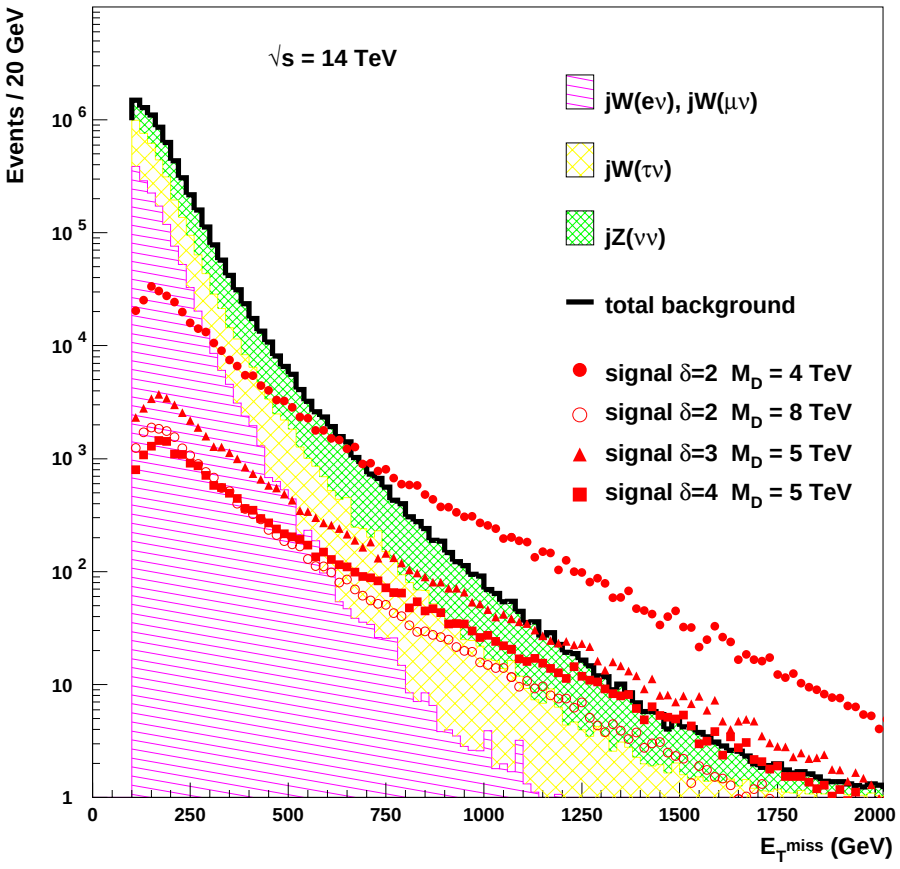

Figure 2. Distribution of the missing transverse energy in background events and in signal events after the selection and for 100 fb^{-1}. The contribution of the three main kinds of background is shown as well as the distribution of the signal for several values of (δ, M_D).

Type	Low luminosity, $30 fb^{-1}$	High luminosity, $100 fb^{-1}$
$jZ(\nu\nu)$	153	523
$jW(\tau\nu)$	45	151
$jW(e\nu)$	4	12
$jW(\mu\nu)$	4	14
Total	206	700

Table 1. Number of remaining background events after the selection $\not\!\!E_T > 1$ TeV.

δ	M_D	Low luminosity, 30 fb^{-1}			High luminosity, 100 fb^{-1}		
	(TeV)	Events	$\mathcal{S}_{min}$	$\mathcal{S}_{max}$	Events	$\mathcal{S}_{min}$	$\mathcal{S}_{max}$
2	4	1024	27.0	71.4	3465	49.6	131.1
	5	423	11.1	29.5	1430	20.5	61.4
	6	203	5.4	14.1	681	9.7	25.8
	7	110	2.9	7.7	366	5.2	13.8
	8	64	1.7	4.5	212	3.0	8.0
	9	40	1.1	2.8	135	1.9	5.1
	10	27	0.7	1.9	88	1.3	3.3
3	4	643	17.0	44.9	2161	30.9	81.2
	5	212	5.6	14.8	705	10.1	26.7
	6	85	2.2	5.9	288	4.1	10.9
	7	39	1.0	2.8	131	1.9	5.0
	8	20	0.5	1.4	68	1.0	2.6
4	4	448	11.8	31.3	1499	21.4	56.7
	5	117	3.1	8.1	391	5.6	14.8
	6	39	1.0	2.7	134	1.9	5.1
	7	16	0.4	1.1	53	0.8	2.0

Table 2. Number of remaining signal events after the selection ($\not{E}_T > 1$ TeV) and statistical significances.

The sensitivity we quote for M_D is derived from this curve and is the maximum value of M_D such as:

- $\mathcal{S}_{max} > 5$
- at least 100 signal events
- $E^{jet}_{T_{cut}} > 1$ TeV

Hence the sensitivities for two, three and four extra-dimensions are respectively $M_D^{max} = 9.1$, 7.0 and 6.0 TeV. For 30 fb^{-1} collected in 3 years of running at low luminosity, and with a cut on the minimal number of signal events relaxed to 50, the best reachable values of M_D are 7.7:6.2:5.2 TeV for δ =2:3:4.

5. Single photon signature

Another interesting signal at LHC is the production of the graviton in association with a photon. However the rates are much lower than in the jet case and the region of (δ, M_D) which can be probed is much more limited. We include a discussion here as this signature could be used as a confirmation after a discovery in the jet channel. The rates in this channel will be predicted once the jet signal is observed.

5.1. Effective theory and validity range

To determine the validity range of the theory, we used the same method as described in section 2.4. For two extra-dimensions, we observe large differences between the standard cross-section and the truncated one ($\hat{s} < M_D^2$) for M_D below 4 TeV, clearly showing that the predictions are model dependent in this range. Unfortunately, the rates for $M_D \geq 4$ TeV are very low. For three extra-dimensions, there is no region

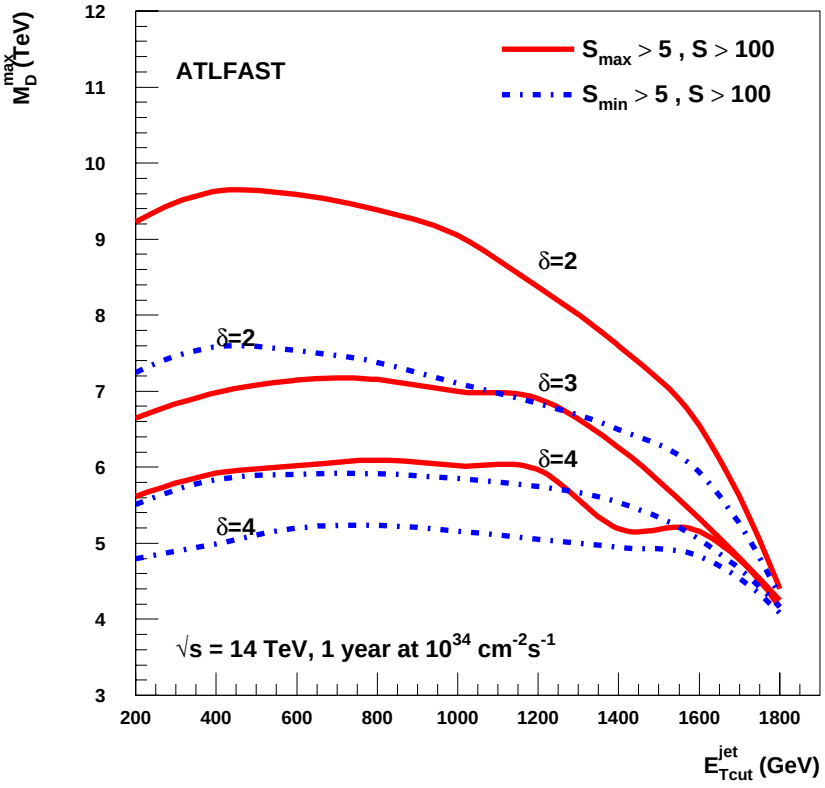

Figure 3. Maximum reach in M_D by selecting events with a jet of $E_T > E_{T_{cut}}^{jet}$ for the standard significance of $\mathcal{S}_{max} > 5$ and for the conservative significance of $\mathcal{S}_{min} > 5$. 100 fb^{-1} of luminosity is assumed. The inflection of the curves for $E_T \sim 1400$ GeV is an artefact of the requirement of having at least 100 signal events and the convergence around 1800 GeV is due to the fall-off of the cross-section for the signals.

where model independent predictions can be made and where the rate is high enough to observe signal events over the background. The situation is of course even worse for larger values of δ.

5.2. Backgrounds

The main Standard model background is γZ where the Z decays into two neutrinos. PYTHIA 5.720 [16] has been used to generate 300k events. As in the jet case, the second most important background is the channel where a W boson is produced with the photon and where a large amount of missing energy can appear because of the W decay to $\tau\nu$. Since the number of events with the other leptonic decays of the W

($e\nu$ and $\mu\nu$) which survived the lepton veto has been found to be negligible for the jet channel, those backgrounds have not been simulated for the photon channel.

5.3. Analysis

For triggering, at least one photon with $E_T > 60$ GeV at high luminosity and within $|\eta| < 2.5$ is required as well as at least 100 GeV of missing transverse energy. In addition, the lepton veto described in section 4.3.2 has been applied. As before the signal emerges from the background at large transverse missing energy: typically $\not\!\!E_T > 500$ GeV is required.

5.4. Signal significance

For an integrated luminosity of 100 fb^{-1} and after requiring that $\not\!\!E_T > 500$ GeV, the number of remaining events for $\delta = 2$ and $M_D = 4$ TeV is 61.8. The number of background events is 82.9: 80.7 for $\gamma Z(\nu\nu)$ and 2.2 for $\gamma W(\tau\nu)$, leading to a significance $\mathcal{S}_{max} = 6.8$.

To derive the conservative sensitivity, a calibration sample of $\gamma Z(ee)$ events has been generated and selected as follows: in addition to a photon fulfilling the same trigger requirements as above, two electrons within $|\eta| < 2.5$ and with $p_T > 20$ GeV/c are required. The invariant mass of the two electrons has to lie within $m_Z \pm 10$ GeV. The calibration sample is 6 times smaller than the background sample. Therefore the statistical estimator used is $S/\sqrt{6B}$ and the significance is $\mathcal{S}_{min} = 2.8$.

As expected the sensitivity is limited with this channel. Nevertheless it could provide a valuable check in case of a discovery in the jet channel, provided both the number of extra dimensions and the mass scale are not too large.

6. Determination of the number of extra-dimensions

If a signal is observed at LHC, one would like to measure the fundamental parameters M_D and δ. The direct graviton emission processes discussed in this note are in particular more attractive for finding the number of extra dimensions of the theory than the processes with virtual graviton exchange where the dependency on δ is weak. In the following, a method to do so is discussed qualitatively.

Using only the shape of the $\not\!\!E_T$ spectrum (cf. figure 2), it is not possible to determine both δ and M_D; for instance the signal for $\delta = 2$ and $M_D = 6$ TeV is very similar to the one for $\delta = 3$ and $M_D = 5$ TeV. In order to distinguish these, one could exploit the variation of the cross-section with the center of mass energy of the LHC: there is a kinematic limit on the partonic subprocess which implies a limit on the largest value of the emitted graviton mass. The ratio of cross-sections at different center of mass energies is almost independent of M_D and varies with δ. Provided the error is small enough, measuring this ratio should allow a determination of the number of extra-dimensions.

The study of the single jet signature was repeated for a center-of-mass energy of the LHC of 10 TeV, assuming an integrated luminosity of 50 fb^{-1}. The $\delta = 4$ case is no longer accessible. However, the rates for ($\delta = 2, M_D = 6$ TeV) and ($\delta = 3, M_D = 5$ TeV) now differ by approximately a factor of two. We found that an experimental accuracy of 5% on the ratio $\sigma(pp \to jG)_{\sqrt{s}=10\ TeV}/\sigma(pp \to jG)_{\sqrt{s}=14\ TeV}$ is needed to discriminate between $\delta = 2$ and $\delta = 3$. For $M_D = 6$ TeV and $\delta = 2$, the event rate at

δ	$\sqrt{s} = 14$ TeV 100 fb^{-1}	$\sqrt{s} = 14$ TeV 1000 fb^{-1}	$\sqrt{s} = 28$ TeV 100 fb^{-1}	$\sqrt{s} = 28$ TeV 1000 fb^{-1}
2	9	12	15	19
3	7	8	12	14
4	6	7	10	12

Table 3. 5-sigma discovery limits on M_D (TeV) for various scenarios.

10 TeV is approximately 1/3 of that at 14 TeV and, since the event rates are small, comparable integrated luminosity would actually be needed to measure the rate with sufficient statistical accuracy. Note also that the relative luminosity of the LHC at the two energies would also need to be measured with comparable accuracy.

The relatively high integrated luminosity required for such a measurement is obviously a limitation since running at $\sqrt{s} = 10$ TeV for a long period of time would certainly not be possible. However the method could be used after a luminosity or energy upgrade as discussed in section 7.

7. Sensitivity beyond LHC

While the LHC is the natural place to probe the multi-TeV region which is the prime territory of this large extra-dimension model, a higher energy/luminosity collider would allow the exploration of even larger ranges for M_D and δ. Three different scenarios have been considered: an order of magnitude increase of the luminosity to 10^{35} cm^{-2}s^{-1}, doubling the center-of-mass energy to 28 TeV, or both. The reader is referred to reference [17] for a general discussion of the impact on the physics capabilities of the ATLAS detector in such scenarios.

This kind of physics is relatively immune to changes in the detector layout which might be required to operate with an enhanced collider (the luminosity upgrade being obviously the most demanding one): only the calorimeter is really needed, the eventual removal of the inner detector for instance is not expected to have a significant impact. Furthermore the signal involves high p_T jets and large $\not\!\!E_T$, being for that reason insensitive to possible drastic increases of thresholds at the trigger level.

For each of these scenarios, a study of the single jet channel, the most promising one, has been performed in a similar way as the one for the nominal parameters of LHC. The 5-sigma discovery limits on M_D for these scenarios are summarized in table 3. It can be seen that doubling the center-of-mass energy approximately doubles the reach in M_D. Unfortunately the rates for $\delta > 4$ would still be too low.

Since the best significance in the $\sqrt{s} = 28$ TeV case is obtained with a cut on the $\not\!\!E_T$ of the order of 1 TeV like in the $\sqrt{s} = 14$ TeV case, doubling the energy also doubles the minimal value of M_D below which the calculation becomes unreliable: rate changes and new signals may appear below $M_D^{min} \sim$ 7,8 and 10 for respectively $\delta = 2, 3$ and 4. The main drawback of this is that the overlap region where one can try to determine the number of extra-dimensions by comparing the signals for $\sqrt{s} = 14$ and 28 TeV as explained in section 6 is very limited, at least for a simple analysis (one can still play with the $\not\!\!E_T$ cut to maximize this region, provided the background remains under control): basically one would be able only to distinguish $\delta = 2$ from $\delta = 3$ and only if $M_D \sim 8$ TeV. On the other hand, if a signal is observed at 14 TeV, model dependent signals are very likely to appear at 28 TeV and would be very

valuable to understand the underlying theory.

8. Conclusion

The generic missing transverse energy signals for theories having large extra dimensions have been studied. The most promising signature is the one where a a jet accompanies the large missing energy caused by the emission of the Kaluza-Klein states into the extra dimensions. For such a process and after one year of running at the design luminosity, the LHC can probe the mass scale of the theory up to 9, 7 and 6 TeV if there are respectively two, three or four extra dimensions. This corresponds to a radius of the compactified space between a few micrometers and a picometer. The prospects after the initial three-year run at low luminosity are of the same order, typically 1 TeV below the high-luminosity reach. Running the LHC at a different center-of-mass energy could help to find out the number of extra dimensions. An eventual collider with $\sqrt{s} = 28$ TeV would approximately double the sensitivity on the mass scale and furthermore would provide very valuable insight into the dynamics of the underlying theory if a signal is observed at 14 TeV, since model dependent signals should then appear at 28 TeV.

Acknowledgments

This work has been performed within the ATLAS Collaboration, and we thank collaboration members for helpful discussions. We have made use of the physics analysis framework and tools which are the result of collaboration-wide efforts.

Special thanks to F.Paige for his help in implementing the extra dimensions processes in ISAJET and to G.Azuelos for careful reading of this article.

This work was supported in part by the Director, Office of Science, Office of High Energy and Nuclear Physics, of the U.S. Department of Energy under Contract DE-AC03-76SF00098. Accordingly, the U.S. Government retains a non-exclusive, royalty-free license to publish or reproduce the published form of this contribution, or allow others to do so, for U.S. Government purposes.

References

[1] Arkani-Hamed N, Dimopoulos S and Dvali G 1998 *Phys. Lett.* **B429** 263
[2] Antoniadis I 1990 *Phys. Lett.* **B246** 377
[3] Green M B, Schwarz J H and Witten E 1987 *Superstring Theory* vol 1 (Cambridge, Uk: Univ. Pr.) and references therein.
[4] Giudice G F, Rattazzi R and Wells J D 1999 *Nucl. Phys.* **B544** 3
[5] Paige F and Protopopescu S 1986 *Supercollider Physics* ed. Soper D (World Scientific) p 41
[6] Baer H, Paige F, Protopopescu S and Tata X 1993 *Proc. Workshop on Physics at Current Accelerators and Supercolliders* ed. Hewett J, White A and Zeppenfeld D (Argonne National Laboratory)
[7] Cullen S and Perelstein M 1999 *Phys. Rev. Lett.* **83** 268
[8] Lai H L, Botts J, Huston J, Morfin J G, Owens J F, Qiu J, Tung W K and Weerts H 1995 *Phys. Rev.* **D51** 4763
[9] ATLAS Collaboration 1999 *Detector and Physics Performance Technical Design Report* CERN/LHCC/99/14-15
[10] Richter-Was E, Froidevaux D, and Poggioli L 1998 *ATLFAST 2.0: a fast simulation package for ATLAS* ATLAS Internal Note ATL-PHYS-98-131
[11] ATLAS Collaboration 1998 *First-Level Trigger Technical Design Report* CERN/LHCC/98/14
[12] ATLAS Collaboration 1998 *DAQ, EF, LVL2 and DCS Technical Progress Report* CERN/LHCC/98/16

[13] ATLAS Collaboration 1998 *Trigger Performance Status Report* CERN/LHCC/98/15
[14] ATLAS Collaboration 1999 *Detector and Physics Performance Technical Design Report* CERN/LHCC/99/14 Section 9.2.2
[15] Vacavant L and Hinchliffe I 2000 ATLAS Internal Note ATL-PHYS-2000-016 and hep-ex/0005033
[16] Sjostrand T 1994 Comput.Phys.Commun. **82** 74-90
[17] Azuelos G *et al.* 2000 ATLAS Internal Note ATL-COM-PHYS-2000-030